Electronic Supplementary Material (ESI) for Inorganic Chemistry Frontiers.

Electronic Supplementary Information

Kinetic Separation of C_2H_6/C_2H_4 in A Cage-Interconnected Metal-Organic Framework: An Interaction-Screening Mechanism

Mo Xie, Zhou Lu,† Weigang Lu,* Dan Li*

College of Chemistry and Materials Science, Guangdong Provincial Key Laboratory of Functional Supramolecular Coordination Materials and Applications, Jinan University, Guangzhou, Guangdong 510632, People's Republic of China.
E-mail: weiganglu@jnu.edu.cn; danli@jnu.edu.cn
†Present address: Department of Chemistry, University of North Texas, Denton, Texas 76203, USA.

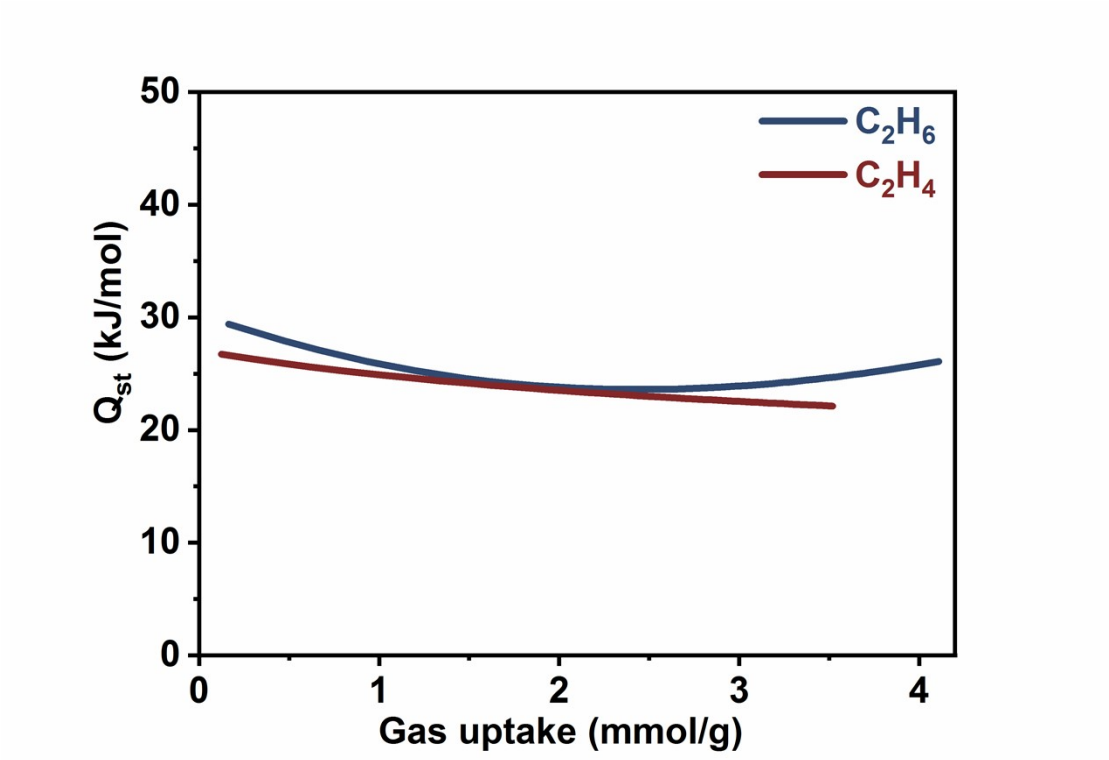

Figure S1. Adsorption enthalpy (Q_{st}) of C_2H_6 and C_2H_4 on **JNU-2** calculated from their experimental adsorption data.

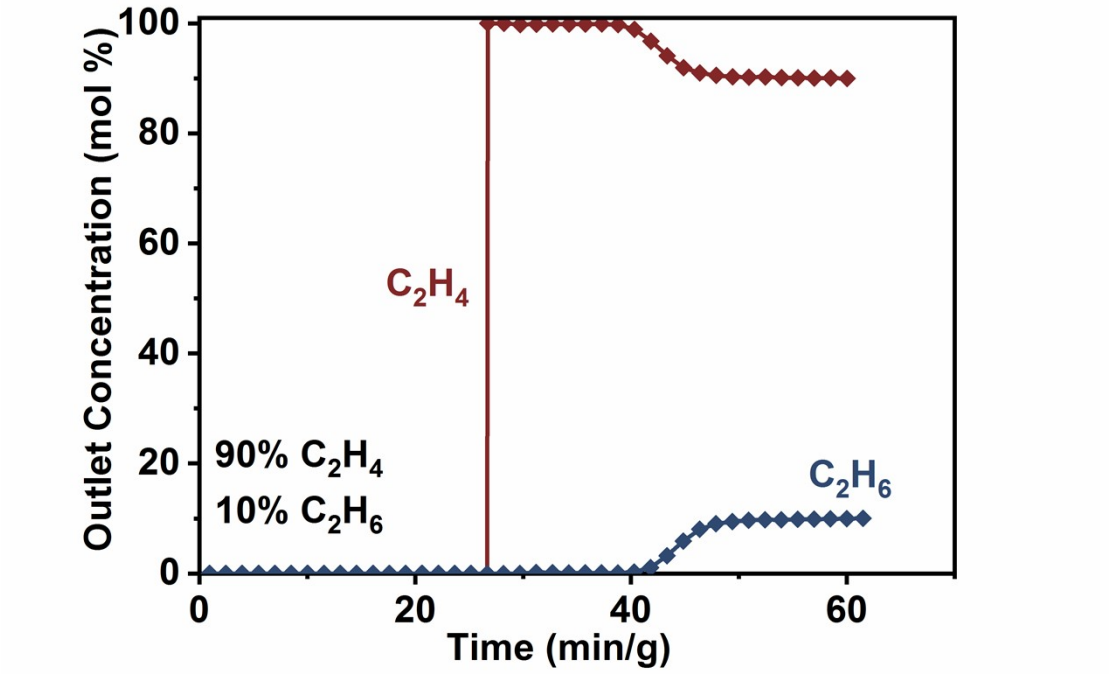

Figure S2. Breakthrough curves for C_2H_6/C_2H_4 (10/90) mixtrue on **JNU-2**.

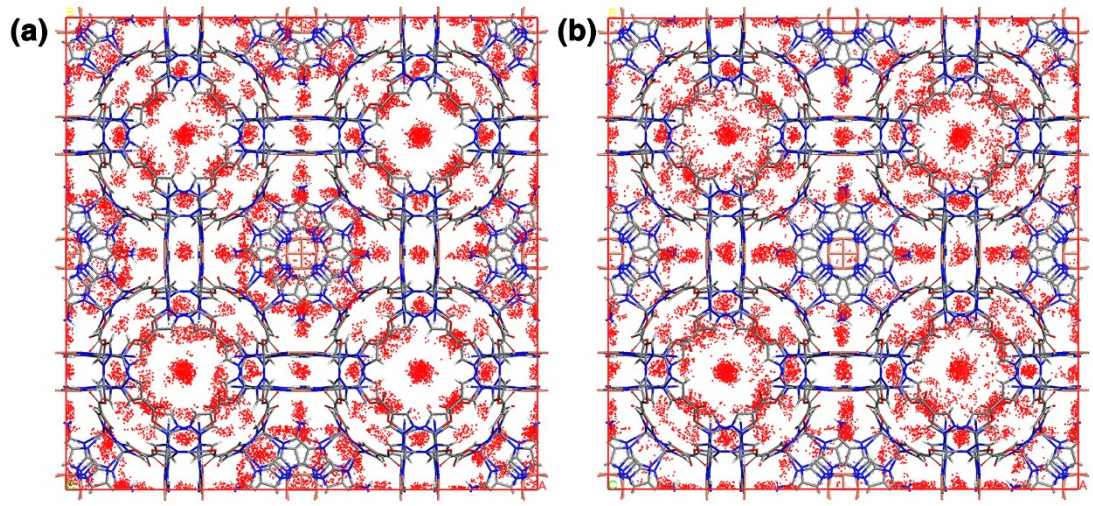

Figure S3. Molecular distribution of C_2H_6 (a) and C_2H_4 (b) in **JNU-2** at 1 bar.

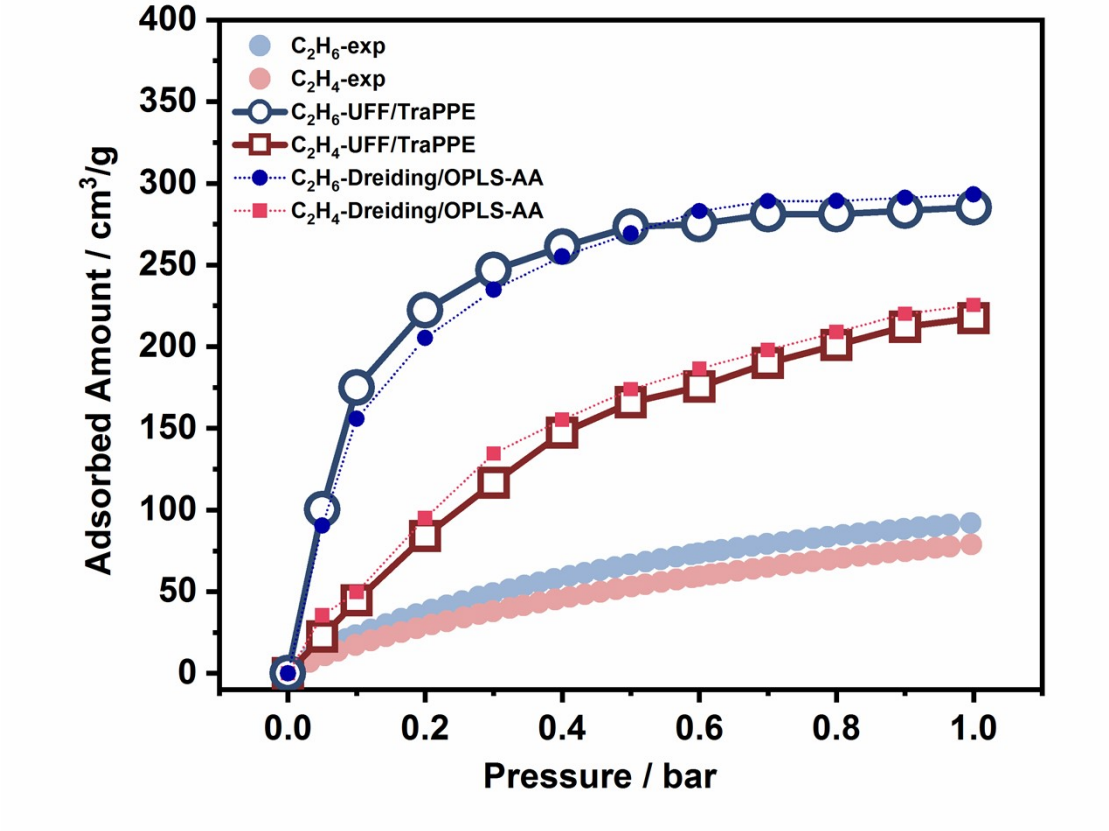

Figure S4. Comparison of the simulated adsorption amount employing different force field parameters.

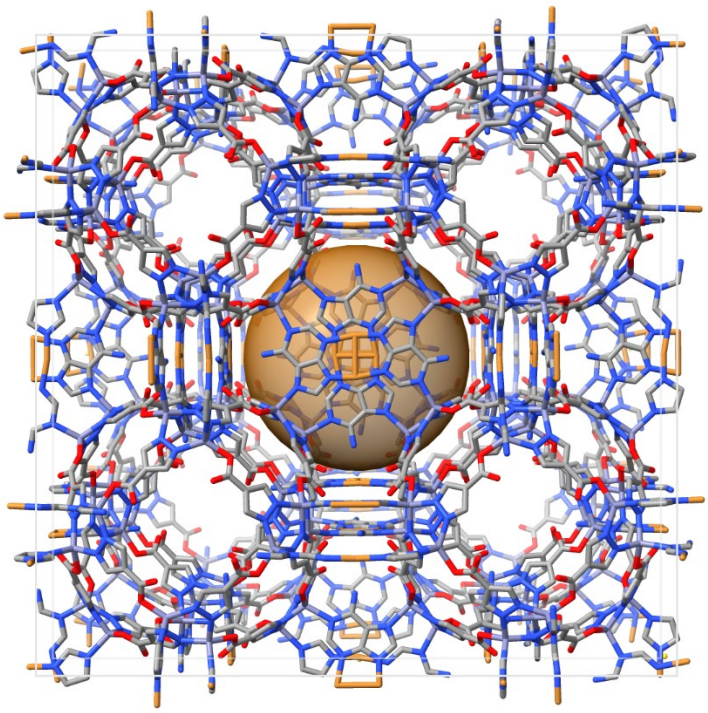

Figure S5. JNU-2 model used in GCMC simulation in the RASPA program, the brown ball represents the blocking sphere.

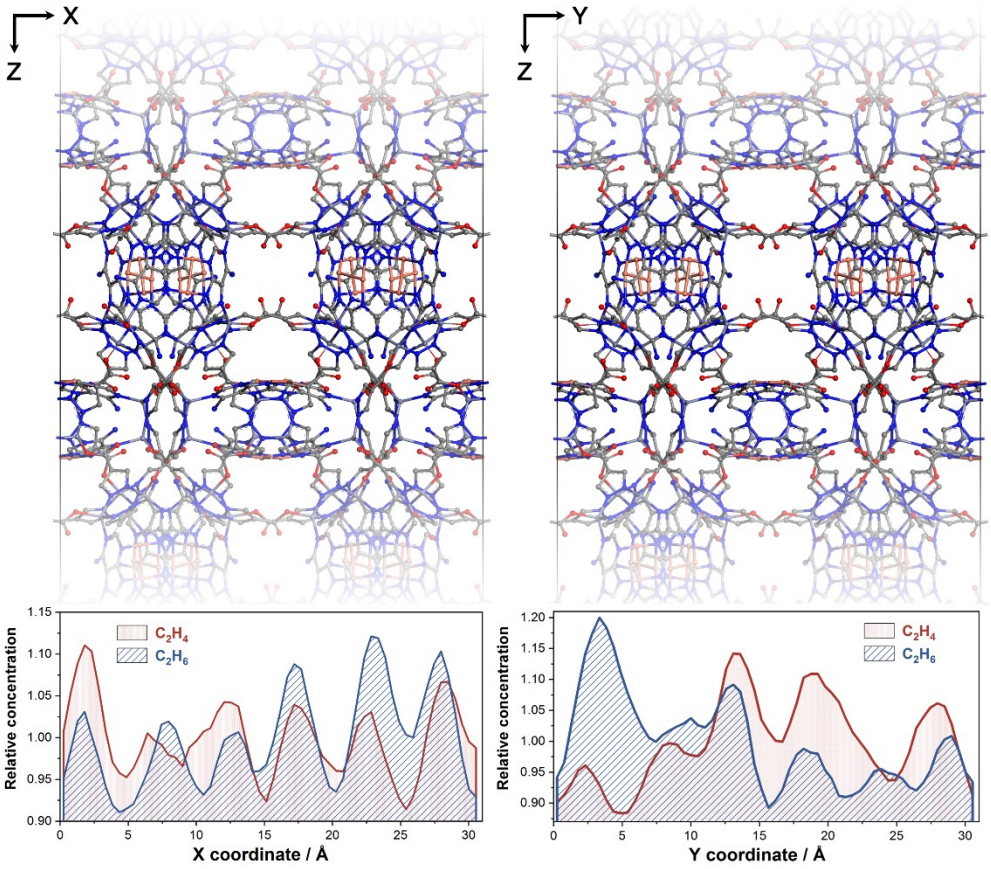

Figure S6. View of **channel I** model in x and y direction, and the statistical gas concentration along X coordination and Y coordination, respectively.

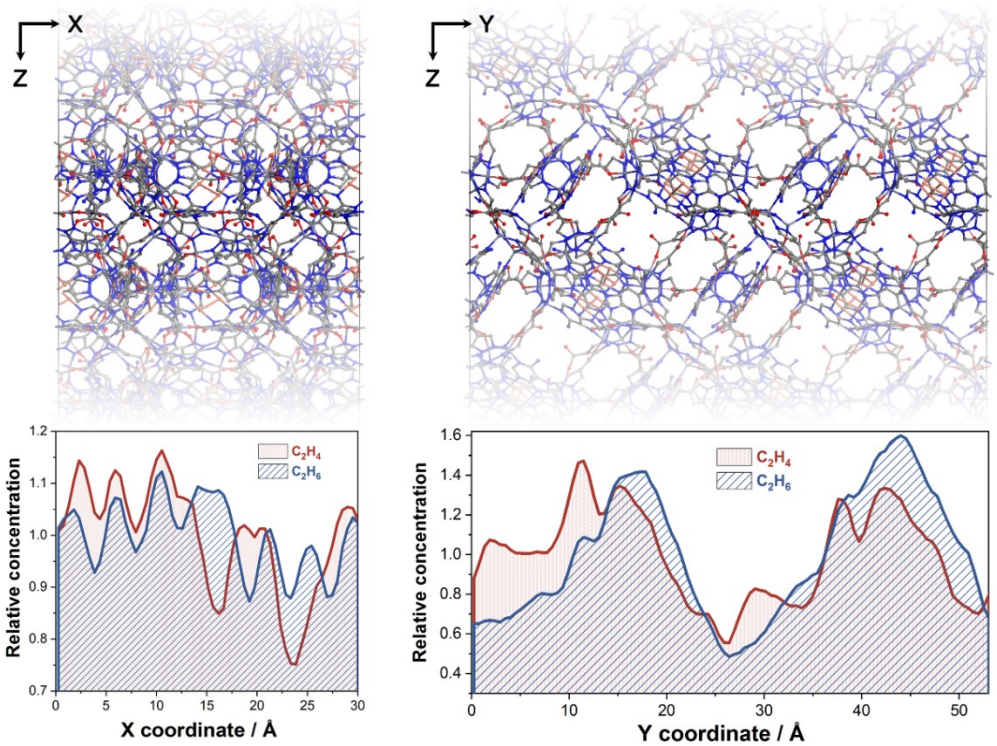

Figure S7. View of **channel II** model in x and y direction, and the statistical gas concentration along X coordination and Y coordination, respectively.

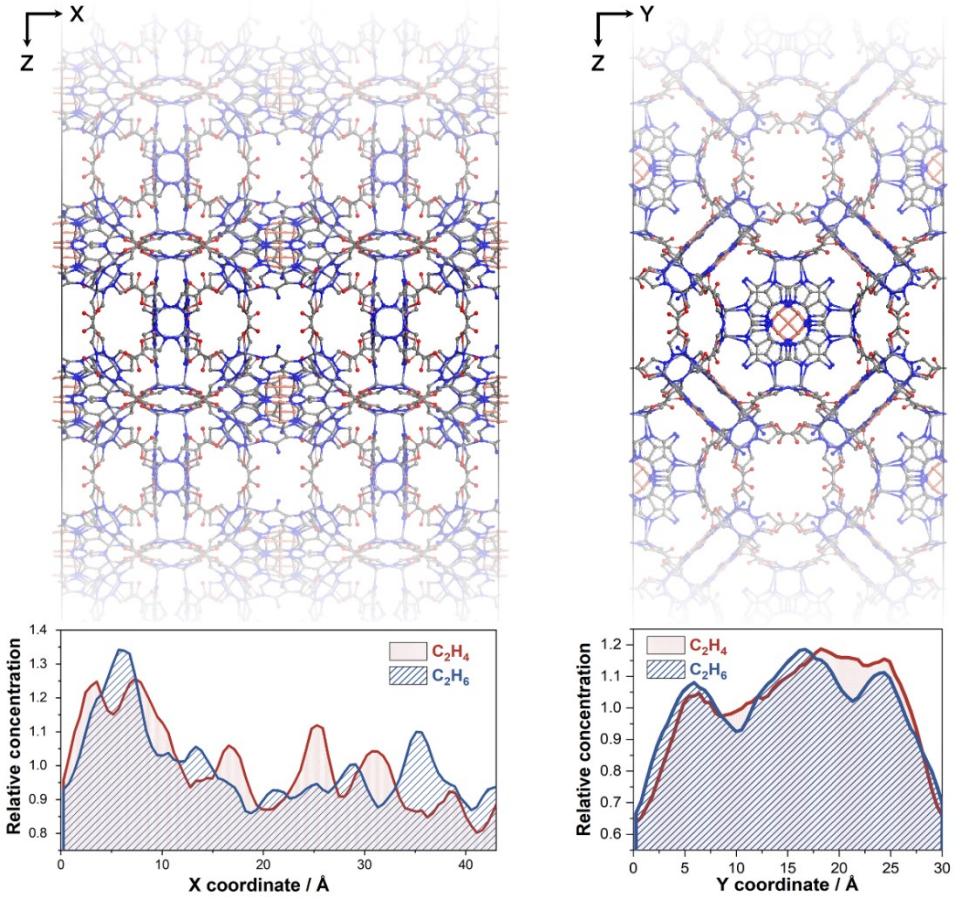

Figure S8. View of **channel III** model in x and y direction, and the statistical gas concentration along X coordination and Y coordination, respectively.

Table S1. The energy decomposition analysis (EDA) of the interaction energy between $5C_2H_4$/$5C_2H_6$ and **Cage B**.

	$5C_2H_4$ / kcal/mol	$5C_2H_6$ / kcal/mol
E_{ele}	-37.90	-33.64
E_{rep}	74.63	67.00
E_{orb}	-13.98	-14.75
E_{disp}	-54.85	-49.57
E_{total}	-32.11	-30.97

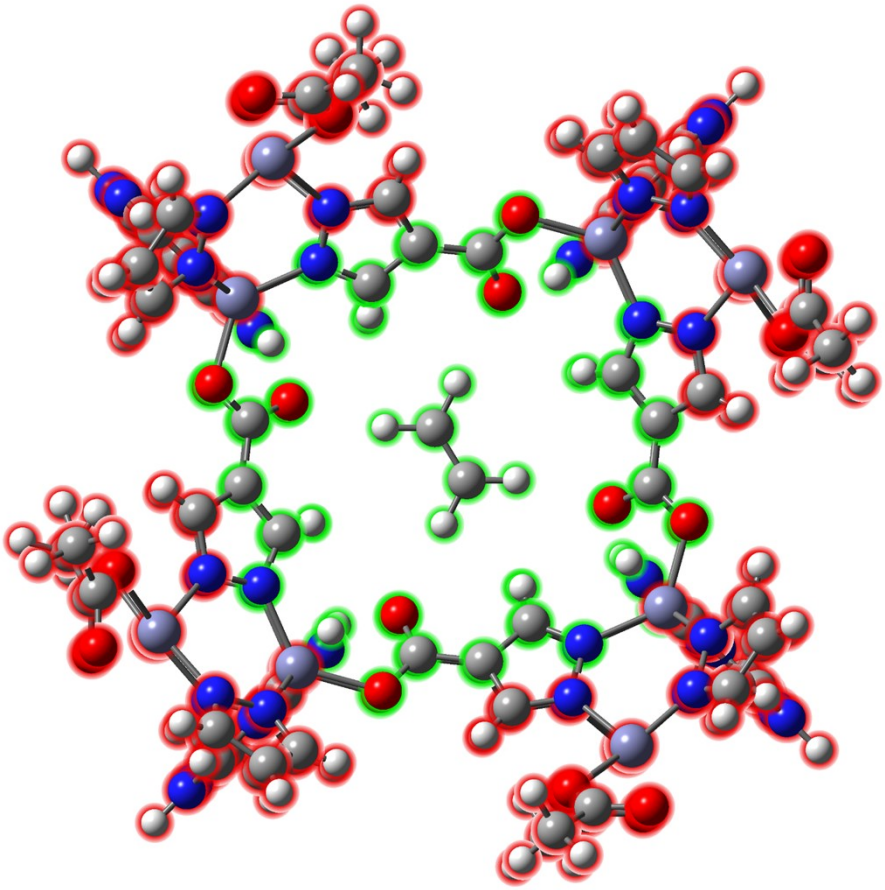

Figure S9. Schematic diagram of gas@**Cage A** model (take C_2H_4@**Cage A** as an example) used in DFT calculations, fixed atoms are labelled in red, and unfixed atoms are labelled in green.

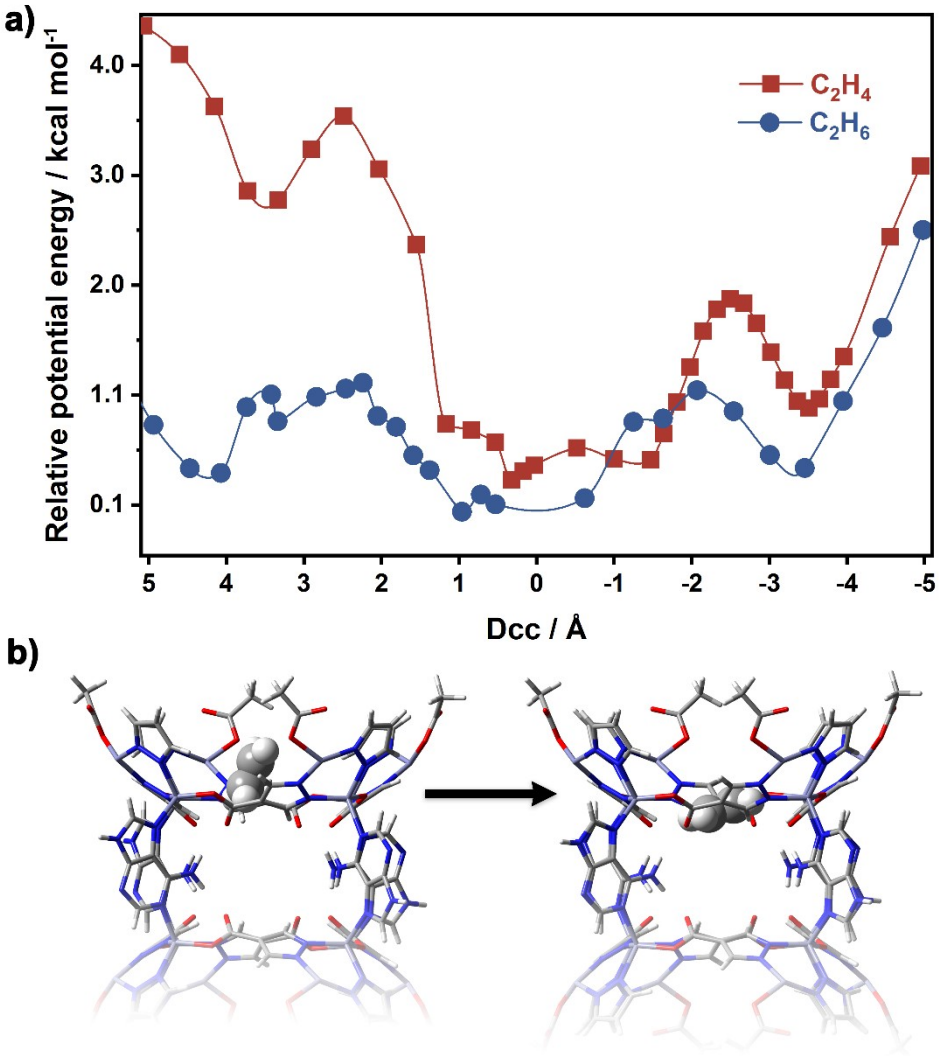

Figure S10. a) The relative potential energy curve of gas molecules moving along the axis of Dcc. Dcc is displayed as negative when gas molecules are moving away from the center of **Cage A**. C_2H_4 is in a vertical configuration when approaching **Window 1**, and changes into a parallel configuration in the middle of **Window 1**. This could be the reason for the higher potential energy of C_2H_4 in the Dcc range of 5.0~1.0 Å.

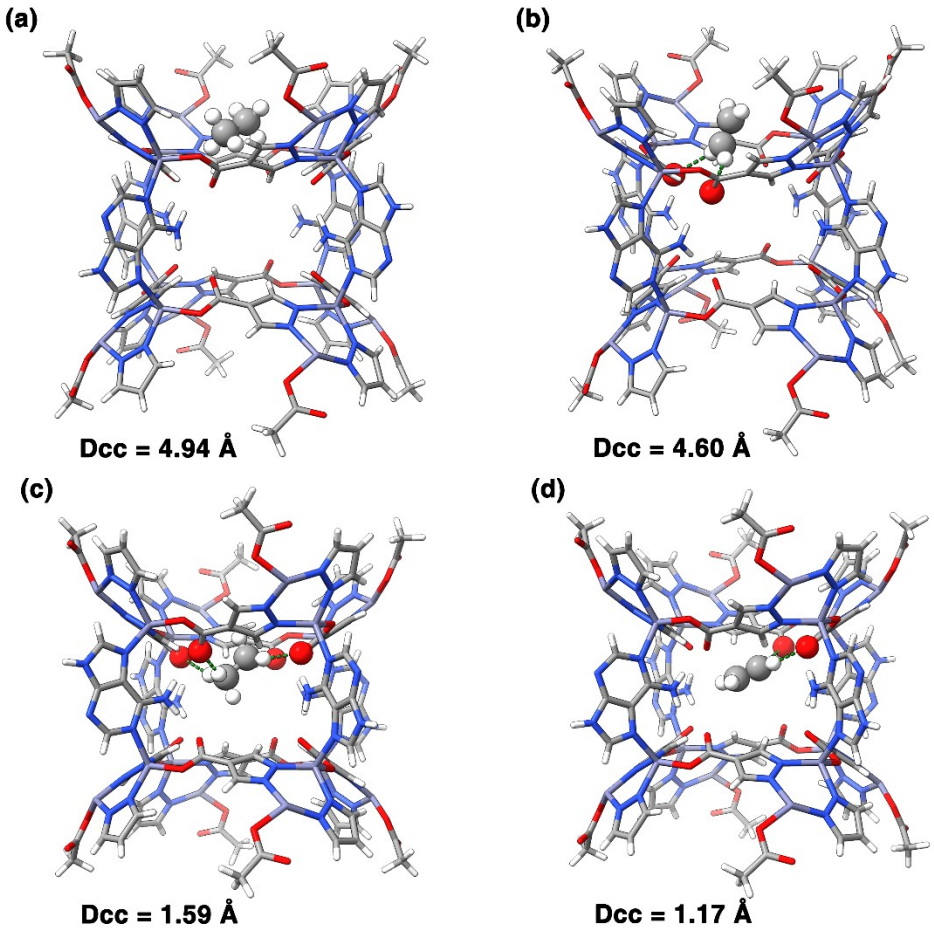

Figure S11. The interaction configurations of C_2H_6 and C_2H_4 at **Cage B** edge (a and b) and entering **Cage A** center (c and d), the corresponding Dcc are shown.

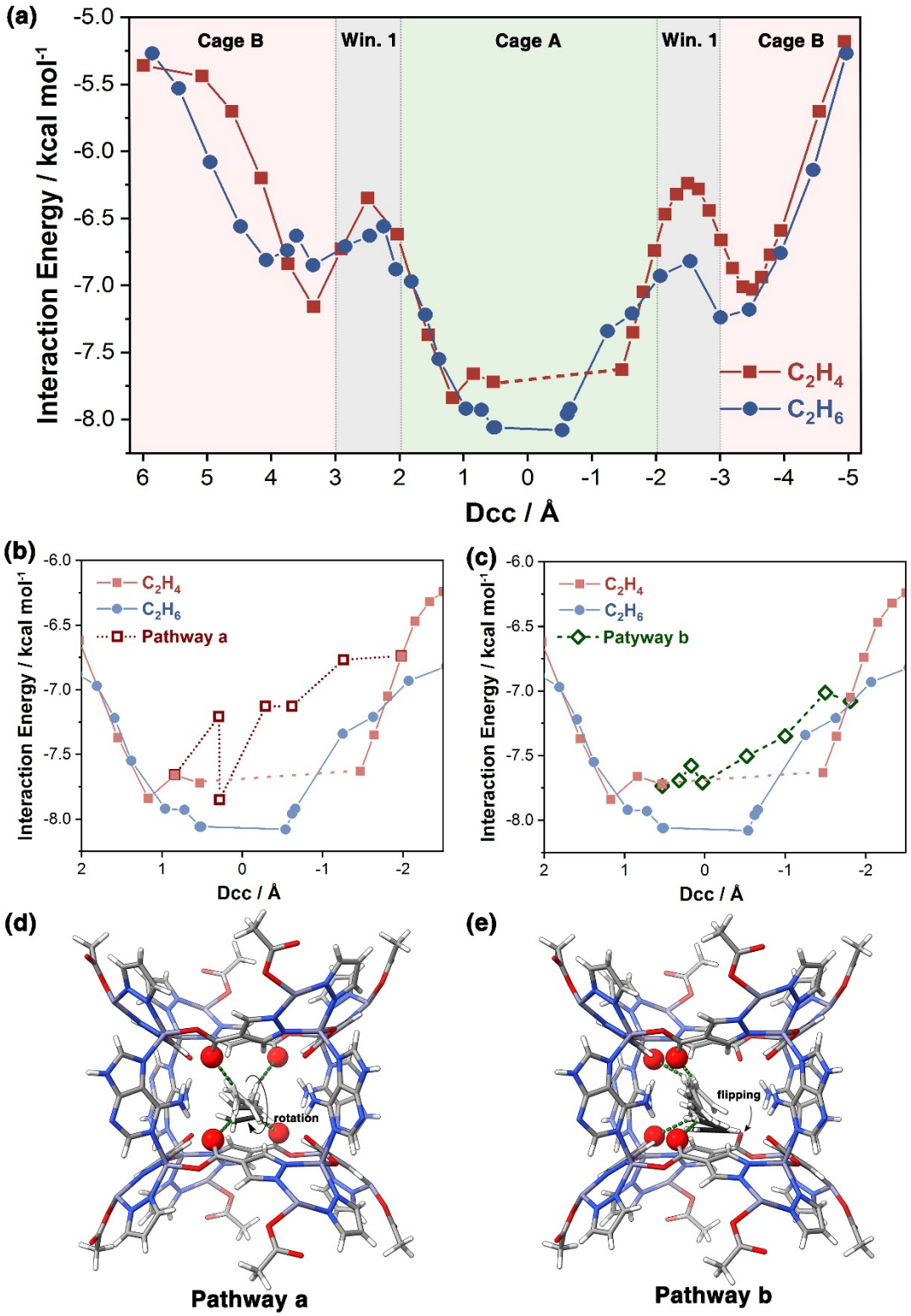

Figure S12. The interaction energy profile (a) of actual calculations in which the center of C_2H_4 cannot move continuously on the z-axis with the **Cage A** center as the origin. The proposed C_2H_4 pathways (b and c) based on hydrogen-bonding interaction and the C_2H_4 molecular position change (from light grey to dark grey) of the proposed pathway a (rotation, d) and b (flipping, e). The molecular motion and potential hydrogen bonds are shown as well.

Discussion:

During the relaxed scanning calculation, we attempt to make the center of gas molecules move continuously along the z-axis with the **Cage A** center as the origin. The results show that C_2H_6 can move continuously according to the established route in steps of 0.5 Å while C_2H_4 cannot do this in the range between Dcc = 1 and Dcc = -1. If put the C_2H_4 molecule in the middle of **Cage A** and optimize the C_2H_4@**Cage A** interaction structure, we can obtain two different geometries both with four hydrogen bonds, in which the C_2H_4 center is offset from the **Cage A** center in the x-direction or y-direction. Herein, two possible pathways were proposed which enable C_2H_4 to continue the movement by keeping four hydrogen bonds, and the scanned interaction energy and schematic diagram of two pathways were shown in Figure S9b-e. In pathway a, the C_2H_4 molecule flip 90º with the C-C bond as the axis, which is approximately perpendicular to the plane of **Window 1**. As shown in Figure S9d, C_2H_4 molecule can form four hydrogen bonds with the two opposite oxygen atoms of the upper and lower windows. In pathway b, the C_2H_4 molecule keeps the upper two hydrogen atoms stationary and forms two hydrogen bonds with two adjacent oxygen atoms of the lower **Window 1** by rotating to the side of **Cage A**. The two cis hydrogen atoms interact with the para-oxygen atoms of the upper or lower bottom of **Window 1**, generating a total of four hydrogen bonds. The energy barriers of pathway b are smaller than that of pathway a, indicating pathway b is more reasonable and adopted as part of the interaction energy curve for C_2H_4 in the main text.

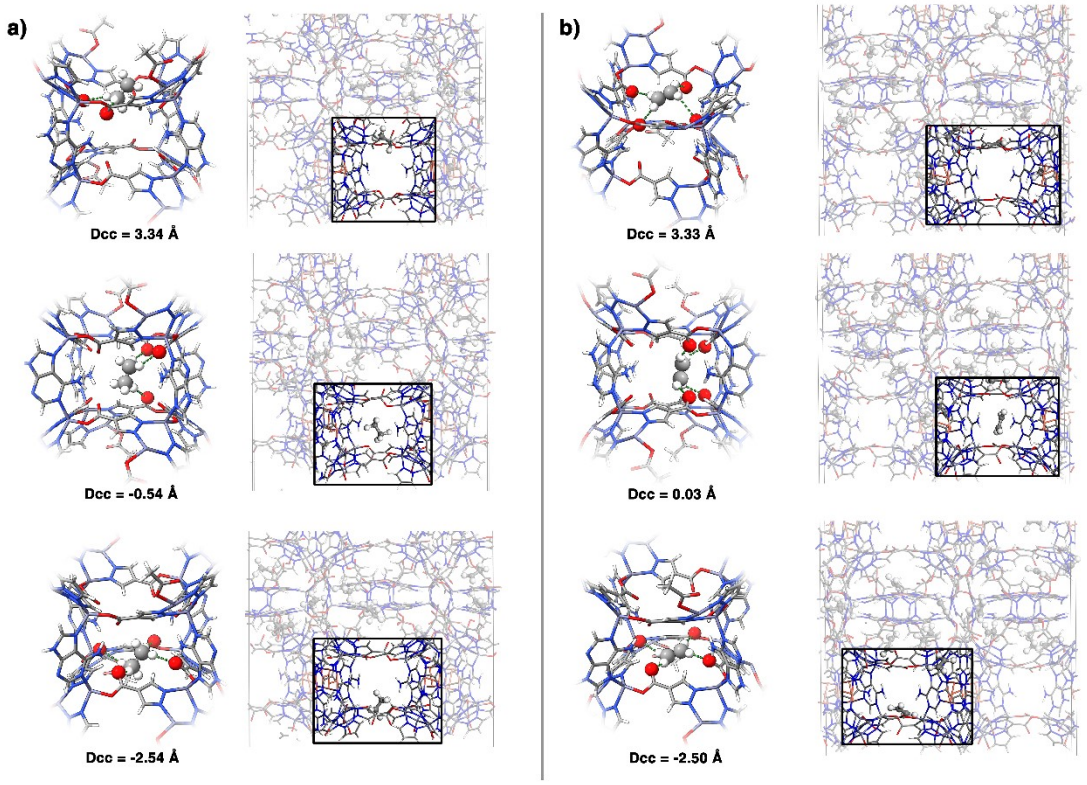

Figure S13. The representative interaction configurations of C_2H_6@**Cage A** (a) and C_2H_4@**Cage A** (b) from DFT calculations and their similar configurations observed in **Channel I** from MD simulations.

Table S2. DFT calculated NBO (natural bond orbital) atomic charge of C_2H_6 and C_2H_4.

molecule	atom	atomic charge / e
C_2H_6	C	-0.587
	H	0.196
C_2H_4	C	-0.377
	H	0.188